Insights into the binding of the drugs diclofenac sodium and cefotaxime sodium to serum albumin: Calorimetry and spectroscopy

ARTICLE *in* EUROPEAN JOURNAL OF PHARMACEUTICAL SCIENCES: OFFICIAL JOURNAL OF THE EUROPEAN FEDERATION FOR PHARMACEUTICAL SCIENCES · MARCH 2012

Impact Factor: 3.35 · DOI: 10.1016/j.ejps.2012.03.007 · Source: PubMed

3 AUTHORS, INCLUDING:

Sinjan Choudhary
Centre for Excellence in Basic Sciences
14 PUBLICATIONS **48** CITATIONS

SEE PROFILE

European Journal of Pharmaceutical Sciences 46 (2012) 435–445

Contents lists available at SciVerse ScienceDirect

European Journal of Pharmaceutical Sciences

journal homepage: www.elsevier.com/locate/ejps

Insights into the binding of the drugs diclofenac sodium and cefotaxime sodium to serum albumin: Calorimetry and spectroscopy

Ruchika Sharma, Sinjan Choudhary, Nand Kishore *

Department of Chemistry, Indian Institute of Technology Bombay, Powai, Mumbai 400 076, India

ARTICLE INFO

Article history:
Received 7 February 2012
Received in revised form 15 March 2012
Accepted 20 March 2012
Available online 29 March 2012

Keywords:
Bovine serum albumin
Diclofenac
Cefotaxime
Calorimetry
Binding thermodynamics
Spectroscopy

ABSTRACT

Understanding physical chemistry underlying drug–protein interactions is essential to devise guidelines for the synthesis of target oriented drugs. Binding of a non-steroidal anti-inflammatory drug, diclofenac sodium (DCF) and an antibiotic drug, cefotaxime sodium (CFT) belonging to the family of cephalosporins with bovine serum albumin (BSA) has been examined using a combination of isothermal titration calorimetry (ITC), differential scanning calorimetry (DSC), steady state and time resolved fluorescence and circular dichroism spectroscopies. Binding affinity of both DCF and CFT with BSA is observed to be of the order of 10^4 M^{-1}, with the binding profiles fitting well to the single set of binding site model. The disagreement between calorimetric and van't Hoff enthalpies indicates non-adherence to a two-state binding process which could be attributed to changes in the conformation of the protein upon ligand binding as well as with increase in the temperature. Circular dichroism and the fluorescence results, however, do not show any major conformational changes upon binding of these drugs to BSA, and hence the discrepancy could be due to temperature induced conformational changes in the protein. The results of ionic strength dependence and binding in the presence of anionic, cationic and non-ionic surfactants indicate, involvement of more that a single type of interaction in the binding process. The ITC results for the binding of these drugs to BSA in presence of each other indicate that the binding sites for the two drugs are different, and therefore binding of one is not influenced by the other. The DSC results provide quantitative information on the effect of these drugs on the stability of serum albumin. The combined calorimetric and spectroscopic approach has provided a detailed analysis including thermodynamics of the binding of DCF and CFT with BSA qualitatively and quantitatively.

1. Introduction

It is imperative to understand the molecular basis of drug–protein interactions because it greatly influences the biological activity of a drug. The knowledge of the nature and magnitude of drug–protein binding can help us understand and also modulate the pharmacokinetics and pharmacodynamics of a drug. Once introduced into the system, drugs are bound to various blood constituents like cells, proteins, etc. Within the plasma proteins serum albumin is the most important carrier for a broad spectrum of exogenous and endogenous ligands (Kratochwil et al., 2002). Since the therapeutic effect of a drug is directly related with the free concentration of drugs in the plasma (Briand et al., 1982), it is of central pharmacological interest to study the drug–albumin binding. Detailed knowledge of the drug binding site can provide necessary information about the distribution of the drug in the body, its usage along with the other drugs and other competitive natural catabolites (Brodersen et al., 1988). Serum albumins, being present in very high concentration (~40 mg ml^{-1}) in the blood plasma are the major macromolecules chiefly responsible for maintaining the blood osmotic pressure and the pH (He and Carter, 1992; Peters, 1996). Serum albumin often increases the apparent solubility of hydrophobic drug in plasma and modulates its delivery to cells in vivo and in vitro (He and Carter, 1992). Serum albumin has two major albumin binding sites as described by Sudlow and co-workers (Sudlow et al., 1975, 1976). Site I, also called as the warfarin binding site to which drugs such as warfarin, azapropazone and phenylbutazone bind, is located in subdomain IIA of human serum albumin (Sugio et al., 1999). Site II, which is known as benzodiazepine binding site is located in subdomain IIIA and binds several indole derivatives and benzodiazepines with a high degree of structural specificity (Muller and Wollert, 1979; Sjoholm et al., 1979). Site I has been characterized as a larger binding area consisting of overlapping sites of warfarin and azapropazone (Fehske et al., 1981), and the drugs which usually bind to this site are more bulky heterocyclic molecules. On the other hand, site II is more of a narrow hydrophobic binding pocket and the drugs which bind to it are aromatic carboxylic acids, largely ionized at

* Corresponding author. Tel.: +91 2225767157; fax: +91 2225767152.
E-mail address: nandk@chem.iitb.ac.in (N. Kishore).

0928-0987/$ - see front matter © 2012 Elsevier B.V. All rights reserved.
http://dx.doi.org/10.1016/j.ejps.2012.03.007

physiological pH (Chamouard et al., 1985). Consequently, a clear understanding of the interaction of a drug with serum albumin, and characterization of the binding interactions gives us information which is essential for the rational drug-design process.

Diclofenac sodium (DCF) (monosodium 2-[(2,6-dichloroanilino) phenyl acetate]), a non-steroidal anti-inflammatory drug [NSAID] (Fig. 1), is known for its high biological activity and possesses high potential against pain and rheumatic inflammations (Brogden et al., 1980). It is used as an effective antipyretic and analgesic against acute febrile sore throat and also relieves episodic tension-type headache even at low doses (Kenawi, 2006). Its pharmacological effects are attributed to the inhibition of the conversion of arachidonic acid to prostaglandins, which are the mediators of the inflammatory processes (Jobin and Gagnon, 1971). Moser and co-workers (Moser et al., 1990) have suggested that the high activity of DCF is due to its geometry; the 69° twist that exists between the two phenyl rings, which are tilted at ~109°. Binding of DCF with serum albumins has been reported in literature (Rahman et al., 1993; Dutta et al., 2006), the detailed energetics of binding and effect on the conformation of proteins is not available.

Cefotaxime sodium (CFT) (Fig. 1), commonly known as claforan, belongs to the family of broad spectrum antibacterial drugs called cephalosporins. It has an active nucleus of β-lactam ring which results in a variety of antibacterial and pharmacologic characteristics and is widely used to treat gonorrhea, meningitis, pneumococcal, staphylococcal and streptococcal infections. Its antibacterial activities result from the inhibition of mucopeptide synthesis in the cell wall of mainly gram negative bacteria. There are previous reports in the literature where this class of antibiotics was found to bind to serum albumin with diverse affinity, however, there are discrepancies in the published results (McNamara et al., 1990; Tawara et al., 1992; Nerli et al., 1997; Briand et al., 1982; Markovich and Avereva, 1985).

Several interactions between antibiotics and NSAIDs have been described in the literature and they suggest that anti-inflammatory drugs could increase antibiotic efficacy by altering their pharmacokinetics (Catella-Lawson et al., 2001; Tsivou et al., 2005; Joly et al., 1998; Marks, 1991; Rocca and Petrucci, 2012). Conversely, some antibiotics are able to alter metabolism and/or kinetics of some NSAIDs (Rocca and Petrucci, 2012). In fact, enhancement of the therapeutic effect of some of the cephalosporins has been reported in the presence of DCF (Joly et al., 1998; Marks, 1991; Rocca and Petrucci, 2012). DCF and CFT are the drugs which could be administered together, because of the wide spectrum of diseases they cover, so it is of interest to study their binding efficacy in presence of each other, to the serum albumin. In the present study, ITC has been used to quantitatively determine the thermodynamic parameters accompanying the binding of DCF and CFT with BSA. The nature of interactions involved in the binding process has been investigated by studying the binding as a function of temperature and in the presence of salts and surfactants. The possibility of overlapping binding sites for DCF and CFT has also been examined by conducting combinatorial experiments. The binding has also been studied using fluorescence spectroscopy and compared with the ITC results. The conformational changes in the protein and its stability have been investigated by CD spectroscopy and differential scanning calorimetry.

2. Experimental methodology

2.1. Materials

Fatty acid free BSA, diclofenac sodium salt, cefotaxime sodium salt, sodium chloride, sodium dodecyl sulfate (SDS), triton X-100 (TX-100) and hexadecyl trimethyl ammonium bromide (HTAB) were purchased from Sigma–Aldrich Chemical Co., USA. A Sartorius BP 211D digital balance of 0.01 mg readability was used for the mass measurements. The water used for preparing the solutions was double-distilled and further deionized using a Cole-Parmer research mixed-bed ion exchange column. All the experiments were performed at pH 7.0 in 10 mM phosphate buffer. The protein stock solutions were prepared by extensive overnight dialysis at 4 °C against the buffer. The reported pH is that of the dialysate measured on a Standard Control Dynamics pH meter at room temperature. The concentration of BSA was determined on a Shimadzu double-beam UV 265 spectrophotometer at 280 nm using the extinction coefficient value corresponding to $A^{1\%}_{1cm} = 6.8$ (Sober and Harte, 1973).

2.2. Isothermal titration calorimetry (ITC)

Experiments on binding interaction of the drugs with BSA were done on a VP-ITC titration microcalorimetry system (MicroCal, Northampton, MA). All solutions were thoroughly degassed before use by stirring under vaccum in a Thermovac unit supplied with the instrument. The sample cell was loaded with 0.045 mM protein solution or buffer. The titrations were carried out using a 250 μL autopipet, filled with the respective drug solution (0.675 mM DCF or 1 mM CFT), keeping the stirring speed fixed at 300 rpm. Each experiment consisted of 10 μL consecutive injections of the drug solution at durations of 20 s each with a 4-min interval. Control experiments were performed at the same concentrations of the

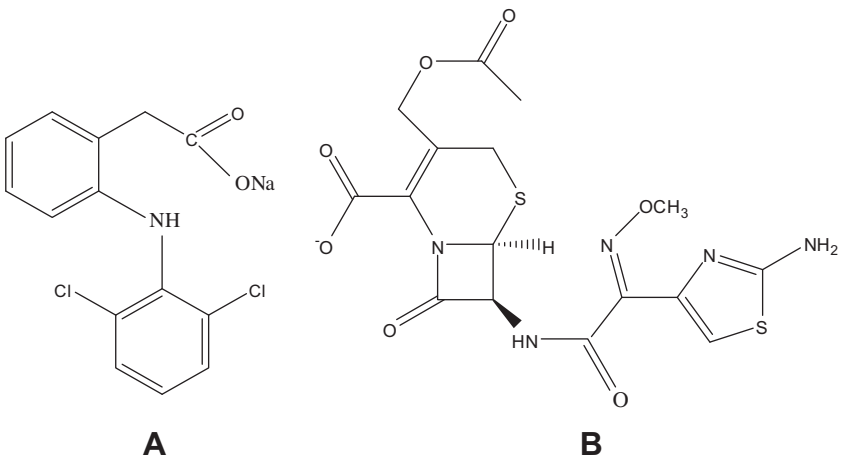

Fig. 1. Structure of diclofenac sodium (A) and cefotaxime sodium (B).

protein and drugs to correct the data for the heats of dilution of the ligand, protein and buffer mixing. For all the experiments, the heat of the binding reaction between the drug and the protein was obtained as the difference between the heat of reaction and the corresponding heats of dilution. The data were analyzed with a single set of identical binding sites model using the Origin 7 software provided by MicroCal.

The plot of change in enthalpy against temperature was used to calculate the value of change in heat capacity upon binding.

2.3. Differential scanning calorimetry

The DSC experiments were performed on Nano DSC (TA-instruments) at scan rate of 1 K min^{-1}. All the solutions were degassed using Barnstead (Thermolyne) from Nuova before loading into the calorimetric vessels. The excess heat capacity scans for the protein transitions were obtained by subtracting the corresponding scans of buffer versus buffer from that of the protein solutions versus buffer. When the experiments were conducted in the presence of drugs, an equivalent amount of drug was added to the reference cell as that present in the protein solution of the sample cell. The DSC data were analyzed by nano-analyzer according to single or multiple transitions.

In order to check the reversibility of denaturation the sample in the first scan was heated to a little over the complete denaturation temperature, cooled immediately and reheated at the same scan rate. It was observed that all the denaturations of BSA in the absence and presence of drugs are irreversible.

2.4. Fluorescence spectroscopy

A Perkin-Elmer model LS-55 spectrofluorimeter was used to measure the intrinsic fluorescence of BSA in the presence of DCF and CFT in a quartz cell of 3 ml capacity and path length of 1 cm. The protein concentration in all experiments was kept at 7.25×10^{-7} mol dm^{-3}. The excitation and emission slits were fixed at 5 nm. The tryptophan residues were selectively excited by keeping the excitation wavelength fixed at 295 nm and the emission spectra were recorded in the wavelength range of 300–400 nm at a scan rate of 10 nm min^{-1}.

2.5. Time-resolved fluorescence measurements

Time-resolved fluorescence measurements were performed at the magic angle using a pulsed Nano-LED based time-correlated single-photon counting fluorescence spectrometer with λ_{ex} = 295 nm from IBH, UK and λ_{em} = 340 nm. The full width at half-maximum of the instrument response function is 250 ps and the resolution is 56 ps per channel. The data were fitted to biexponential function after deconvolution of the instrument response function by an iterative reconvolution technique by the IBH DAS 6.0 data analysis software using reduced $\chi 2$ and weighted residuals as parameters for goodness of the fit.

2.6. Circular dichroism (CD) spectroscopy

CD spectra in the far- (190–260 nm) and near-UV (260–320 nm) regions were obtained on a JASCO-810 spectropolarimeter for observing the alterations in the secondary and tertiary structure of the protein. The protein concentration and path lengths used were 5 μM and 0.2 cm, respectively, for the far-UV CD experiments and 20 μM and 1 cm, respectively, for near-UV CD experiments. The spectropolarimeter was thoroughly purged with nitrogen prior to the experiments. Each spectrum was baseline corrected and was taken as an average of three accumulations at a scan rate of 500 nm min^{-1} and a response time of 1 s. The molar ellipticity $[\theta]$ was calculated from the observed ellipticity θ as

$$[\theta] = 100 \times \left(\frac{\theta}{c \times l}\right) \quad (1)$$

where c is the concentration of the protein in mol dm^{-3} and l is the path length of the cell in centimeters.

3. Results and discussion

3.1. Isothermal titration calorimetry of the binding of DCF and CFT to BSA at various temperatures

3.1.1. Isothermal titration calorimetry of the binding of DCF to BSA

Fig. 2 shows a representative isothermal titration calorimetric profile of the raw signals obtained from the titration of 0.675 mM DCF with 0.045 mM BSA at 25 °C. Each peak in the binding isotherm (Fig. 2, panel A) represents a single injection of the drug into the protein solution. Integration of the area of cell feedback by subtracting the dilution heats of both the ligand and the protein gives the differential curve shown in the bottom panel of Fig. 2, panel B. The amount of heat generated per injection has been shown as a function of the molar ratio of the drug to the protein. A standard nonlinear least-squares regression binding model, involving a single class of non-interacting sites fitted well to the data. As seen in Fig. 2, panel B, the fitting curve (solid line) shows good agreement with experimental data represented by the square symbols. The binding experiments were done in the temperature range of 10–35 °C. The temperature dependence of the thermodynamic parameters accompanying the binding of DCF to BSA is summarized in Table 1. The value of each parameter listed in this table is an average of that obtained in two to three independent

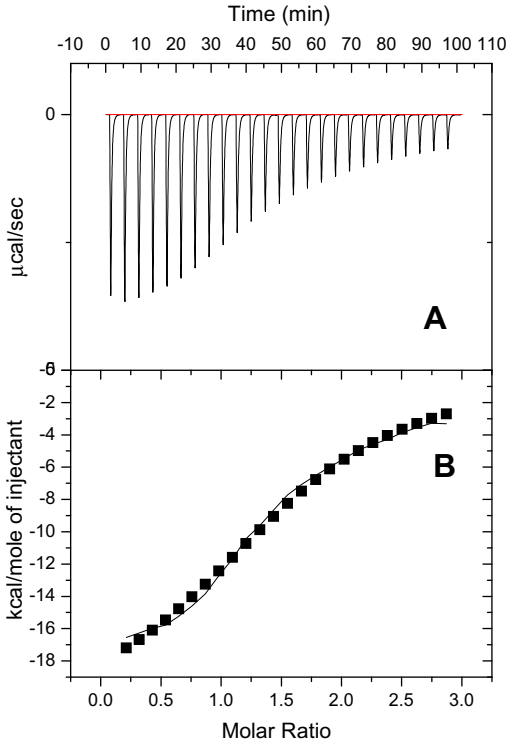

Fig. 2. (A) Raw data for the titration of 0.675 mM DCF with 0.045 mm BSA at 25 °C, showing the calorimetric response as successive injections of the ligand are added to the sample cell. (B) Integrated heat profile of the calorimetric titration shown in panel (A). The solid line represents the best non linear least-squares fit to a single binding-site model.

Table 1
Values of binding constants (K), enthalpy (ΔH) and entropy (ΔS) of binding accompanying the titration of 0.675 mM DCF with 0.045 mM bovine serum albumin at various temperatures.

Temperature (t) (°C)	K (10^4 M^{-1})	ΔH (kcal mol^{-1})	ΔS (cal K^{-1} mol^{-1})
10	2.24 ± 0.50	−58.4 ± 0.10	−186.5
20	4.51 ± 0.40	−22.3 ± 0.09	−54.5
25	6.70 ± 1.10	−24.6 ± 0.08	−60.2
30	5.02 ± 1.00	−15.8 ± 0.09	−30.5
35	5.34 ± 1.10	−19.2 ± 0.12	−40.7

experiments. The observed enthalpy is essentially the binding enthalpy and does not have a significant contribution from the buffer ionization, since phosphate has a small value for the enthalpy of ionization ($\Delta H_{ionization}$ = 3.6 kJ mol^{-1}) (Goldberg et al., 2002). The negative heat of interaction, as seen in Fig. 2, for the ITC titrations of 0.675 mM DCF with 0.045 mM BSA indicates that the binding is an exothermic process with an affinity constant of the order of 10^4 at all the studied temperatures. An increase in the binding affinity, K is observed with rise in temperature from 10 to 25 °C and then it remains nearly the same up to 35 °C. The exothermicity of the binding interaction is observed to be decreasing with increase in temperature. Since both the enthalpy and entropy of binding are observed to be negative, the binding is entropically opposed but enthalpically favored in the studied temperature range.

DCF is a negatively charged molecule at pH 7 (pK_a = 4) (Maitani et al., 1991; Palomo et al., 1999) and is expected to bind at the site consisting of positively charged amino acid residues in the binding cavity of the protein. It is capable of forming hydrogen bonds and inter-molecular charge transfer complex (Kenawi et al., 2005) through the transfer of electrons from the phenyl rings to the positively charged residues on the binding site of the protein. Negative value of the enthalpy of binding suggests that the interaction is mostly electrostatic in nature, the extent of which decreases with rise in temperature. The presence of two aromatic rings in the DCF molecule also provides significant hydrophobic character to the drug. The fall in the negative value of ΔH with rise in temperature suggests enhanced interaction of these hydrophobic groups with the binding site at higher temperature.

3.1.2. Isothermal titration calorimetry of the Binding of CFT to BSA

A representative calorimetric profile for the titration of 1 mM CFT with 0.045 mM BSA at 25 °C is shown in Fig. 3. The titrations were performed at different temperatures and the data thus obtained fitted to a single set of binding site model after fixing the stoichiometry to 1. The value of stoichiometry of binding was established through fluorescence measurements as discussed in Section 3.6. The associated binding parameters are presented in Table 2. The binding interaction is exothermic in nature with an affinity constant of the order of 10^4 at all temperatures. As seen from Table 2, the affinity constant and the enthalpy of binding, do not vary significantly with the change in temperature. Here again, binding is enthalpically favorable but entropically opposed. The value of heat capacity of binding calculated from a plot of ΔH against temperature −(0.04 ± 0.05 kcal K^{-1} mol^{-1}) indicates insignificant alterations in the extent of the exposure of hydrophobic groups to the solvent upon binding.

3.2. Effect of ionic strength and surfactants on the binding of DCF and CFT with BSA

Ionic strength dependence of a biomolecular association can provide insights for assessing the contribution of charge–charge interactions to the binding process (Barcelo and Portugal, 2004). To understand the role of electrostatic interactions in the binding

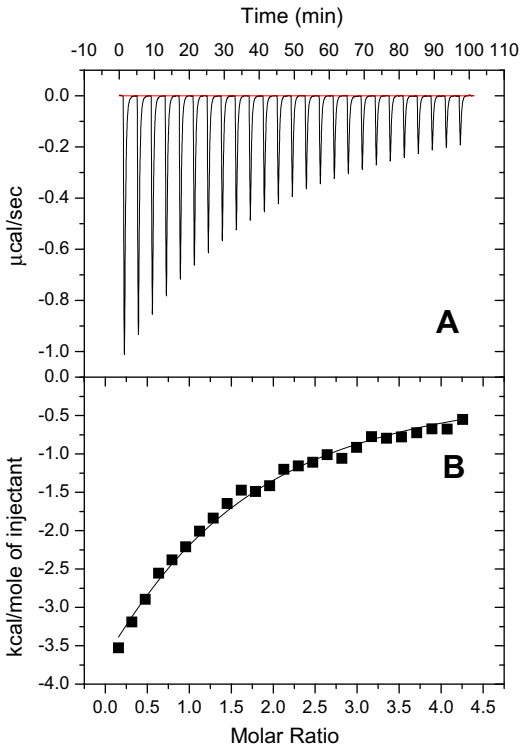

Fig. 3. (A) Raw data for the titration of 1 mM CFT with 0.045 mm BSA at 25 °C, showing the calorimetric response as successive injections of the ligand are added to the sample cell. (B) Integrated heat profile of the calorimetric titration shown in panel (A). The solid line represents the best nonlinear least-squares fit to a single binding-site model.

Table 2
Values of binding constants (K), enthalpy (ΔH) and entropy (ΔS) of binding accompanying the titration of 1.0 mM CFT with 0.045 mM bovine serum albumin at various temperatures.

Temperature (t) (°C)	K (10^4 M^{-1})	ΔH (kcal mol^{-1})	ΔS (cal K^{-1} mol^{-1})
10	1.66 ± 0.19	−7.29 ± 0.22	−6.4
20	1.99 ± 0.40	−6.42 ± 0.59	−2.6
25	1.41 ± 0.26	−8.97 ± 0.61	−11.1
30	1.82 ± 0.38	−8.14 ± 0.68	−7.4
35	1.12 ± 0.88	−7.59 ± 0.58	−6.1

of these drugs to BSA, the ITC experiments were performed in the presence of different concentrations of NaCl at pH 7 and 25 °C. The binding parameters thus obtained are listed in Table 3.

With increase in the concentration of NaCl from 0.05 to 0.5 M, for the binding of DCF to BSA, the binding affinity decreases slightly. The enthalpy and entropy of binding, however, do not

Table 3
Values of binding constants (K), enthalpy (ΔH) and entropy (ΔS) of binding accompanying the titration of 0.675 mM DCF and 1.0 mM CFT with 0.045 mm BSA in the presence of NaCl at 25 °C.

NaCl (M)	N	K (10^4 M^{-1})	ΔH (cal mol^{-1})	ΔS (cal K^{-1} mol^{-1})
DCF				
0.05	2.05	5.08 ± 0.76	(−1.30 ± 0.05) × 10^4	−22.1
0.2	1.96	4.66 ± 0.47	(−1.23 ± 0.04) × 10^4	−20.0
0.5	1.67	3.00 ± 0.34	(−1.60 ± 0.08) × 10^4	−33.2
CFT				
0.05	1.0	1.10 ± 0.23	(−5.33 ± 0.55) × 10^3	0.6
0.1	1.0	0.64 ± 0.32	(−4.84 ± 1.43) × 10^3	1.2
0.25	1.0	0.30 ± 0.12	(−3.59 ± 1.48) × 10^3	3.8

show significant variation with increase in the ionic strength. For CFT, increase in the ionic strength from 0.05 to 0.25 M, also leads to a decrease in the binding affinity as reflected by the decrease in the value of *K*.

For both the drugs the binding is thermodynamically linked to the number of counter ions (Na^+) bound to the protein, through the double logarithmic plot of log*K* against log[Na+] (Barcelo and Portugal, 2004). For DCF, the slope of a double logarithmic plot is −0.2, which is smaller than that obtained in the case of CFT where the slope is −0.8. The value of slope gives the number of counterions released upon drug binding (Record et al., 1978). This indicates that there is a larger contribution of ionic interactions in the binding of CFT to BSA than that of DCF at the same pH.

In order to assess the hydrophobic contribution to the binding of drugs to the protein and also to examine if there is an overlap of binding sites on BSA for the drugs and surfactants, experiments were carried out in the presence of different surfactants at below and above their critical micelle concentrations (CMC) at pH 7 and 25 °C. Figs. S1 and S2 show the ITC profiles obtained for the binding of DCF and CFT to BSA, respectively, in the presence of anionic, cationic and non-ionic surfactants and the corresponding thermodynamic data is given in Table 4. For both the drugs in the presence of the anionic surfactant sodium dodecyl sulfate (SDS) {CMC = 8.2 mM}, no typical binding pattern is observed, below or above its CMC. The partial denaturing capability of SDS (Carter and Ho, 1994) in our studied concentration range is expected to hamper the integrity of the binding sites. Also, due to its anionic nature, SDS interferes with the binding of the drug to the positively charged residues on the protein. Both these factors lead to loss in binding of the drugs, DCF and CFT with BSA. At higher concentrations of SDS hydrophobic interactions also become important. Therefore, at the micellar concentration, it can interfere in the hydrophobic associations of the drugs with BSA.

Based on the equilibrium dialysis and intrinsic fluorescence spectroscopic studies, it has been predicted (Kragh-hansen et al., 2001) that all the domains of serum albumin have the capacity to bind amphipathic dodecyl compounds. Gelamo and co-workers (Gelamo and Tabak, 2000; Gelamo et al., 2002) suggested that the fluorescence quenching observed in the case of SDS binding to BSA was due to direct contact of the surfactant molecule with the indole of Trp 131 residue. Hence, it is obvious that SDS can influence the hydrophobic associations between the ligand and the serum albumin. The fact that SDS is interfering with the binding of DCF and CFT with BSA at below and above its CMC, suggests that hydrophobic as well as electrostatic interactions are playing a vital role in the binding of both these drugs with BSA.

In the presence of cationic surfactant, hexadecyltrimethylammonium bromide (HTAB) at both above and below its CMC (CMC = 0.91 mM) (Takeda et al., 1987), DCF shows a binding profile where the heat signals cross from exothermic to endothermic effects and do not saturate (Fig. S1). Also, it appears that at these concentrations, since a typical binding profile is obtained, the denaturing effect of HTAB does not adversely influence the integrity of binding sites. Similar to this, the interaction of CFT with BSA also do not show zero saturating heat signals (Fig. S2). In this case, at the micellar concentration of HTAB, only endothermic heat signals are observed. This can be attributed to DCF (pK_a = 4.0) (Maitani et al., 1991; Palomo et al., 1999) and CFT ($pK_a \approx 3.4$) (Mandell and Sande, 1990) carrying a negative charge at pH 7, and thus have the ability to form complex with positively charged HTAB, dissociation of which upon addition to protein solution or buffer may be different, leading to a non-zero saturating signal in the binding profile. Unlike SDS, HTAB is not expected to block the binding sites for DCF or CFT via electrostatic interactions even though it can influence the hydrophobic associations of the drug with the protein at the micellar concentration.

Binding of DCF in the presence of a non-ionic surfactant triton X-100 (TX-100) below and above its CMC (CMC = 0.261 mM) (Lopez et al., 1998) is shown in Fig. S1. The enthalpy change becomes less negative and the entropy changes from −60.2 cal K^{-1} mol^{-1} to a lesser unfavorable value of −33.8 cal K^{-1} mol^{-1}. Changes in the values of enthalpy and entropy indicate a reduction in the extent of electrostatic interaction between the ligand and the protein. At a higher concentration of TX-100 (0.35 mM) the most notable change in the binding parameters is the increase in the value of *K*, which now becomes $(1.61 \pm 0.68) \times 10^5$ M^{-1}. The possibility of conformational changes in the protein leading to availability of more hydrophobic surface area at higher concentrations of TX-100 explains increased binding affinity with DCF, showing that the hydrophobic interactions are more significant in DCF–BSA binding interactions.

In the presence of 0.15 and 0.35 mM TX-100, binding of CFT with BSA does not seem to be altered to a great extent (Fig. S2). The binding affinity decreases slightly in the presence of both pre- and post-micellar concentrations and the changes in ΔH and ΔS values are not significant as compared to that in the absence of TX-100. These results indicate that binding interaction between CFT and BSA is largely electrostatic in nature, which is not affected on addition of an uncharged surfactant like TX-100 but is hindered on addition of a negatively charged surfactant like SDS.

3.3. Do DCF and CFT to BSA share the same binding sites?

The binding of DCF with BSA in the presence of CFT and vice versa was also studied to understand if these drugs share common binding sites on the protein. This is expected to provide an insight into the nature of the binding sites and the relative affinity of the

Table 4
Values of binding constants (*K*), enthalpy (ΔH) and entropy (ΔS) of binding accompanying the titration of 0.675 mM DCF and 1.0 mM CFT with 0.045 mM BSA at pH 7 in the presence of surfactants at 25 °C.

Surfactant	Surfactant in the syringe (mM)	*K* (M^{-1})	ΔH (kcal mol^{-1})	ΔS (cal K^{-1} mol^{-1})
DCF				
SDS	4.0[a]	No binding		
	8.5[b]	No binding		
TX-100	0.15[a]	$(4.10 \pm 1.16) \times 10^4$	(−16.4 ± 0.13)	−33.8
	0.35[b]	$(1.61 \pm 0.68) \times 10^5$	(−9.77 ± 0.74)	−9.0
CFT				
SDS	4.0[a]	No binding		
	8.5[b]	No binding		
TX-100	0.15[b]	$(9.44 \pm 1.61) \times 10^3$	(−8.51 ± 0.60)	−10.1
	0.35[b]	$(7.51 \pm 1.28) \times 10^3$	(−8.68 ± 0.82)	−11.4

[a] Below CMC.
[b] Above CMC.

drug for the protein in the presence of each other. Fig. S3 shows the ITC profiles obtained for the binding of DCF to BSA in presence of CFT and vice versa. The drug–protein complex in the sample cell was prepared in the molar ratio of 2:1 and the drug concentration in the syringe was kept the same as that in the case of titration with the protein alone. The thermodynamic parameters obtained on fitting the integrated heat profiles to a single binding site model for both the drugs are summarized in Table 5.

The results show that DCF binds to BSA in the presence of CFT with almost the same binding affinity (within the limits of standard deviation) as that in the absence of CFT. The decrease in exothermicity is observed and the entropy changes favorably to a value of -21.2 cal K^{-1} mol^{-1} in comparison to that at 25 °C in the absence of CFT. Similarly, the data on titrations of 1 mM CFT with DCF–BSA complex fitted to a single-binding-site model, the parameters reflecting a very little change in the binding affinity. Here also, the negative binding enthalpy shows a decrease in its value and the entropy changes more favorably from a negative to a small positive value of 1.5 cal K^{-1} mol^{-1} as compared to that in the absence of DCF. The structures of DCF and CFT (Fig. 1) suggest that DCF can interact via both electrostatic as well as hydrophobic interactions with the protein binding sites, whereas CFT has more number of ionic groups through which it can bind to the protein. The hydrophobic interactions between DCF and BSA in the presence of BSA become more prominent as reflected by the changes in the values of enthalpy and entropy of binding. Similar entropy gain is also observed in the case of CFT binding to DCF–BSA complex which means that the hydrophobic interactions increases when CFT binds to the DCF bound BSA. However, the extent of increase in hydrophobic interactions in the case of DCF binding with CFT–BSA complex is more than that for CFT binding with DCF–BSA complex, as reflected by the corresponding change in enthalpy values from those in the presence of the protein alone. Since the binding affinity for both the drugs do not change appreciably in the presence of the other one, the drugs could possibly be binding at different sites on BSA. The hydrophobic cavity which accommodates the hydrophobic rings of both the drugs might be large enough to induce the hydrophobic interactions of both the drugs with the protein.

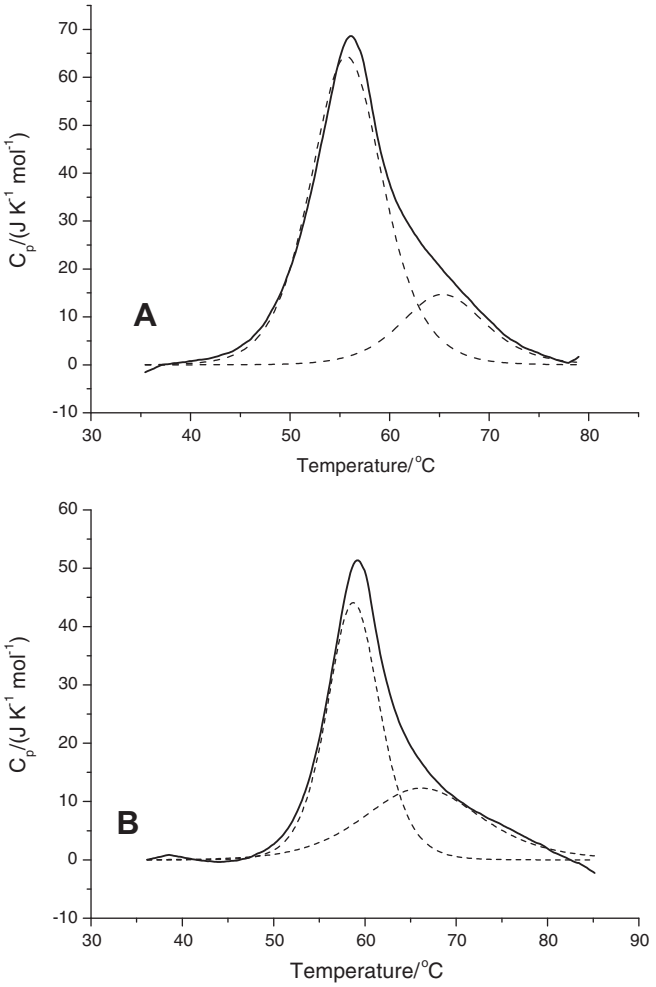

Fig. 4. DSC scans of the thermal denaturation of 0.09 mM BSA at pH 7.4 in presence of CFT at drug to protein molar ratio (A) 1:1, and (B) 50:1 at a scan rate of 1 K min^{-1}.

3.4. Differential scanning calorimetry

Fig. 4 is representative of the DSC scans for BSA thermal denaturation in 20 mM phosphate buffer at pH 7.4 in the absence and presence of CFT. The heat absorption curves shown in this figure correspond to denaturation of BSA solutions having 6 mg ml^{-1} protein. The corresponding thermodynamic parameters accompanying the thermal unfolding of BSA are presented in Table 6. The transition temperature of BSA in the absence of drug is at 55.1 ± 0.1 °C with a transition enthalpy of 80.8 ± 1.4 kcal mol^{-1}. In the presence of CFT a broad transition is observed with a shoulder towards the end of transition (Fig. 4). Upon addition of CFT in 1:1 M ratio of the drug to protein, the overall heat capacity versus temperature curve fits into two components (Fig. 4). The first transition occurs at 55.8 ± 0.1 °C with a transition enthalpy of 91.8 ± 1.7 kcal mol^{-1}. These results indicate that the first transition corresponds to the unfolding of unligated protein and the second transition corresponds to the unfolding of the complexed protein. Upon increasing the molar ratio to 1:5, the transition temperatures of both the components of the main transitions do not change appreciably although the transition corresponding to the ligated protein increases in broadness. Experiments were conducted at higher [CFT]/[BSA] molar ratios (5:1–50:1) (Fig. 4) at the same scanning rate. It is observed that the first component of the transition shows a slow increase in transition temperature. However, the maximum increase in the transition temperature at the maximum studied molar ratio is by 3 K only. The increase in the transition temperature of the first component is accompanied with an increase in the value of enthalpy of unfolding. On the other hand although the transition temperature of the second component remains almost the same, the enthalpy of unfolding decreases with increase in the molar ratio. As observed in fluorescence and ITC measurements, CFT binds to BSA in 1:1 manner. The value of binding constant for the CFT–BSA complex is $(1.41 \pm 0.26) \times 10^4$ at 25 °C which is not indicative of very tight binding. Thus the ligated and unligated protein in the equilibrium mixture results in two components of the main DSC transition even at a very high molar ratio of [CFT] to [BSA]. Increase or decrease in the values of enthalpy of unfolding beyond the stoichiometric ratio may be due to the effect of altered solvent environment.

Fig. 5 represents thermal unfolding of BSA in the absence and presence of DCF. At 1:1 M ratio of DCF to BSA the overall heat

Table 5
Values of binding constants (K), enthalpy (ΔH) and entropy (ΔS) of binding accompanying the titration of DCF and CFT with 0.045 mM BSA at 25 °C.

K (M^{-1})	ΔH (kcal mol^{-1})	ΔS (cal K^{-1} mol^{-1})
Titration of 0.675 mM DCF to CFT–BSA Complex		
$(7.65 \pm 1.67) \times 10^4$	(-13.0 ± 0.05)	-21.2
Titration of 1 mM CFT to DCF–BSA Complex		
$(9.28 \pm 1.25) \times 10^3$	(-5.11 ± 0.36)	1.5

Table 6
Transition temperature (T_m)[a] and enthalpy change (ΔH)[a] associated with the thermal unfolding of 0.09 mM BSA in presence of different concentrations of CFT and DCF at pH 7.4. Subscripts 1 and 2 represent first and second component obtained on deconvolution of the main DSC endotherm.

Molar ratio [drug]/[protein]	T_{m1} (°C)	T_{m2} (°C)	ΔH_1 (kcal mol^{-1})	ΔH_2 (kcal mol^{-1})
Drug: DCF				
1:1	55.8	65.2	91.8	86.3
1:5	56.3	64.9	97.0	81.7
1:10	56.6	65.3	98.5	82.5
1:20	57.4	65.9	102.5	78.2
1:50	58.8	65.5	118.3	55.5
Drug: CFT				
1:1	58.5	66.9	75.8	78.6
1:2	61.5	67.9	71.7	87.2
1:3	66.3	69.8	80.1	98.0
1:5	–	70.5	–	99.4
1:7	–	72.3	–	115.0

[a] The values of T_m and ΔH have an uncertainty of 0.1 K and 2%, respectively.

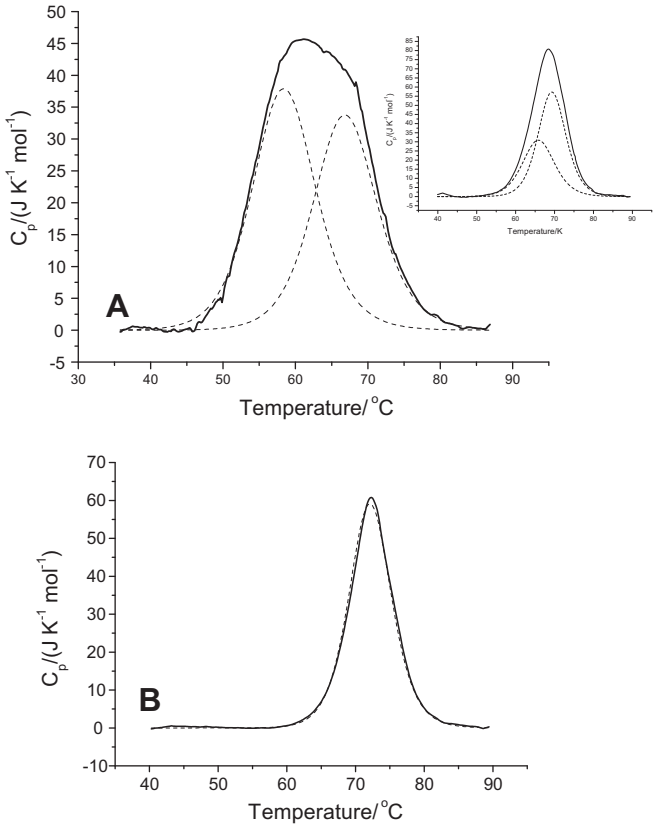

Fig. 5. DSC scans of the thermal denaturation of 0.09 mM BSA at pH 7.4 in presence of DCF at drug to protein molar ratio (A) 1:1, (A, inset) 3:1, and (B) 7:1 at a scan rate of 1 K min^{-1}.

capacity versus temperature curve shows a clear fitting to two components. Here unlike in the case of CFT the co-operativity of the overall transition increases and both the components show an increase in the transition temperature with rise in DCF to BSA molar ratio. The transition temperature of the first component increases from 58.5 ± 0.1 °C at 1:1 M ratio to 66.3 ± 0.1 °C at 3:1 M ratio. The transition temperature of the second component also increases from 66.9 ± 0.1 °C at 1:1 M ratio to 72.3 ± 0.1 °C at 7:1 M ratio. Beyond 3:1 [DCF]/[BSA] molar ratio only one transition is seen (Fig. 5). The increase in the transition temperature of the first component is accompanied with a small change in the transition enthalpy. However the transition enthalpy corresponding to the second transition shows a significant increase from 78.6 ± 1.4 kcal mol^{-1} at [DCF]/[BSA] = 1 to 115.0 ± 2.2 kcal mol^{-1} at [DCF]/[BSA] = 10.

DCF binds to BSA at 25 °C, almost five times more strongly as compared to CFT. The binding enthalpy for DCF is significantly more exothermic compared to that by CFT (Tables 1 and 2). There is also a larger entropy loss associated loss associated with the binding of DCF compared to that of CFT. It is also observed in the DSC studies that the stabilization induced by DCF to BSA is significantly larger than that by CFT. The effect of tighter binding of DCF is further seen in the larger values of enthalpy of denaturation for the second component in overall heat capacity versus temperature curve. The effect of tighter binding in case of DCF is also seen in stronger co-operativity of the DSC transition corresponding to the transition of the complexed protein, which at higher molar ratio gives rise to only one component thermal unfolding profile corresponding to the complexed protein (Fig. 5). The DSC results support tighter binding of DCF with BSA compared to that of CFT and provide a quantitative measure of the thermal stability of the protein in the presence of these drugs.

3.5. Fluorescence spectroscopy

In order to monitor the change in the tryptophan environment of the protein upon binding, the intrinsic fluorescence of 7.25×10^{-7} mol dm^{-3} of BSA in the presence of increasing concentration of drugs was studied. The binding affinity is also calculated for the drug–BSA binding and is compared to that obtained in the ITC experiments for both DCF and CFT. The emission spectra of the protein in the presence of DCF and CFT are shown in Fig. 6. The maximum fluorescence intensity for BSA in buffer alone is observed at 346.5 nm, which matches the value reported in the literature (Kamat and Seetharamappa, 2005).

It was observed that when DCF is added to BSA at different molar ratios a steady decrease in the intensity of the emission maxima takes place with increase in concentration of the drug. However, the value of λ_{max} remains unchanged at all molar ratios of [DCF]/[BSA]. The presence of CFT at different molar ratios with BSA also followed a similar trend of reduced intensity of emission, with a red shift of 2 nm in the λ_{max} at higher molar ratios of [CFT]/[BSA]. These results indicate that the addition of DCF and CFT to BSA causes slight alterations in the tryptophan environment which are located at position 134 and 212 in sub-domains IA and IIA, respectively (He and Carter, 1992; Carter and Ho, 1994).

In order to analyze the quenching of BSA in the presence of the drugs, the Stern Volmer Eq. (2) is used. The bimolecular quenching

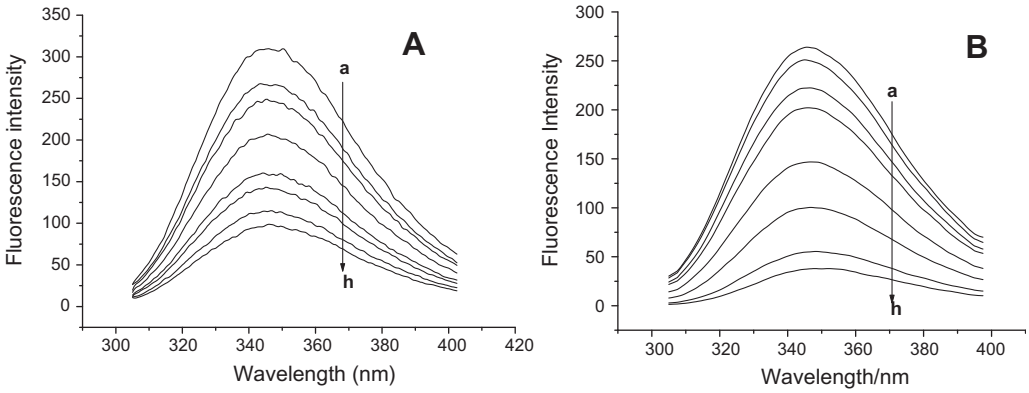

Fig. 6. Intrinsic fluorescence emission spectra of BSA in the presence of (A) DCF at [drug]/[BSA] molar ratio (a) 0:1, (b) 0.26:1, (c) 0.6:1, (d)1:1, (e) 2:1, (f) 3:1, (g) 6:1, (h) 10:1 and (B) CFT at [drug]/[BSA] molar ratio (a) 0:1, (b) 0.5:1, (c) 5:1, (d) 10:1, (e) 25:1, (f) 50:1, (g) 100:1, (h) 138:1.

rate constant was calculated and compared with the limiting diffusion coefficient of the protein which is reported to be, $K_{dif} = 2.0 \times 10^{10}$ L mol^{-1} s^{-1} (Maurice and Camillo, 1981).

$$F_0/F = 1 + k_Q\tau_0[Q] = 1 + K_{SV}[Q] \quad (2)$$

Here F_0 and F are the fluorescence intensities in the absence and presence of the drug, respectively, [Q] is the drug concentration and K_{SV} is the Stern–Volmer quenching constant, which is equal to $k_Q \times \tau_0$, k_Q is the bimolecular quenching rate constant and τ_0 is the average lifetime of the tryptophans in the absence of the drug. Plot of F_0/F against [Q] (Fig. 7) shows a deviation from linearity at higher concentrations of both the drugs which suggests that there is a dynamic contribution to the observed quenching in case of CFT and differing accessibility of tryptophan residues in case of DCF. In the plot of F_o/F versus [Q], an upward curvature form linearity indicates contributions from both the static and dynamic quenching (Eftink and Ghiron, 1976), and the downward curvature indicates differing accessibilities of tryptophan residues (Lehrer, 1971).

The fluorescence lifetime measurement of BSA in the presence of DCF and CFT at different [drug]/[BSA] ratio is done to estimate the extent of dynamic quenching. The lifetime (τ), relative amplitudes (A) and χ^2 of the decay analysis of BSA–DCF and BSA–CFT complexes are tabulated in Table 7. Fig. 8 shows the biexponential fluorescence decay of BSA in the presence of different concentrations of DCF and CFT.

As seen from Table 7, in the presence of DCF there is a sharp decrease in the values of both τ_1 and τ_2 with increase in the [drug]/[BSA] ratio which is reflected by the decrease in the average lifetime as well. Whereas in presence of CFT, the decrease is observed only in the values of τ_2 at higher drug concentrations and hence the average lifetime does not show a large decrease. It is thus inferred, that the binding site for DCF on BSA is located in such a domain that it can quench the tryptophans at positions 134 and 212 more effectively as compared to CFT. Hence the binding sites for both the drugs are not the same.

The linear portion of the plot of F_0/F against [Q] is used to calculate K_{SV} in case of both DCF and CFT. Using Eq. (4), the value of K_{SV}

Table 7
Lifetimes of fluorescence decay of 0.015 mM BSA in the presence of varying [DCF]/[BSA] and [CFT]/[BSA] molar ratios at pH 7.0[a].

[D]/[P]	Lifetime (ns)		Amplitude		Avg. lifetime (ns)	χ^2
	τ_1	τ_2	a_1	a_2	$\langle\tau\rangle$	
DCF–BSA complex						
0	4.12	7.27	0.43	0.57	5.92	1.19
0.5	3.11	6.07	0.46	0.54	4.71	1.06
1	2.37	4.68	0.39	0.60	3.76	1.05
1.5	1.31	3.82	0.27	0.73	3.15	1.12
2	1.07	3.59	0.26	0.74	2.93	1.12
3	0.74	3.32	0.22	0.78	2.76	1.16
5	0.62	3.28	0.26	0.74	2.58	1.09
10	0.42	3.13	0.41	0.59	2.02	1.10
CFT–BSA complex						
0	4.12	7.27	0.43	0.57	5.92	1.19
1	3.48	6.85	0.42	0.58	5.44	1.21
5	2.72	6.28	0.41	0.59	4.82	1.20
10	2.52	6.12	0.43	0.54	4.35	1.15

[a] $I(t) = I(0)[a_1e_1^{-t/\tau} + a_2e_2^{-t/\tau}]$.
where, $a_1 = b_1/(b_1 + b_2)$; $a_2 = b_2/(b_1 + b_2)$; b_1 and b_2 are determined experimentally.
Average lifetime: $\langle\tau\rangle = a_1\tau_1 + a_2\tau_2$.

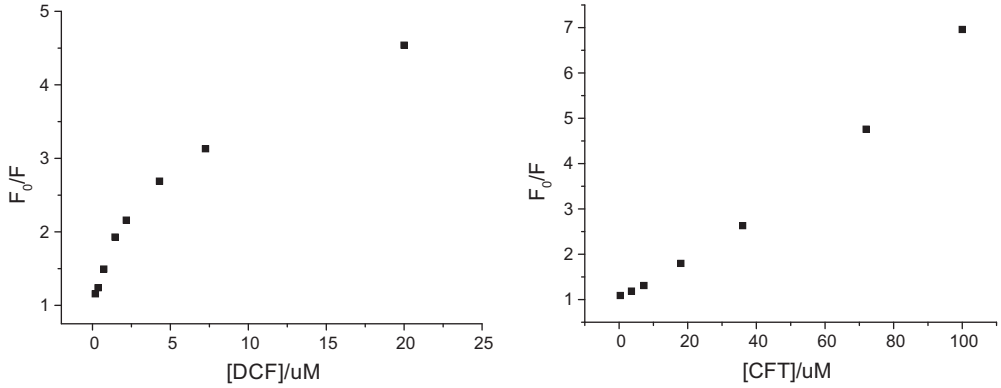

Fig. 7. Plot of F_0/F against the drug concentration.

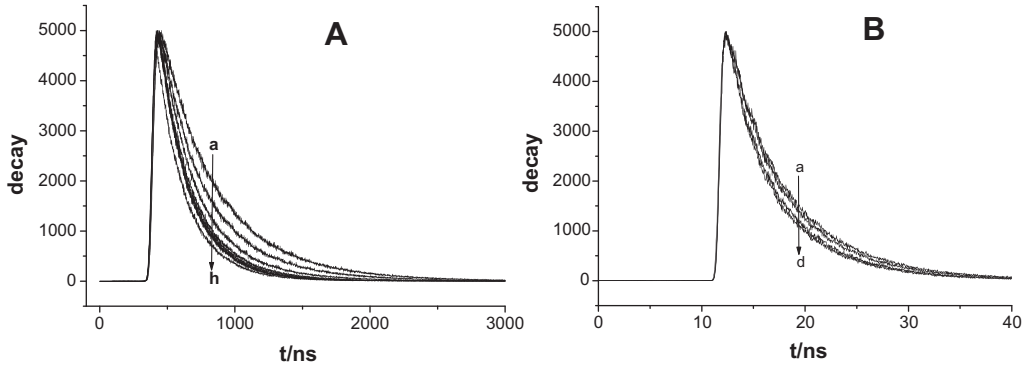

Fig. 8. Fluorescence decay profiles of BSA in the presence of (A) DCF in the molar ratio of 0 (a), 0.5 (b), 1 (c), 1.5 (d), 2 (e), 3 (f), 5 (g), 10 (h) with BSA and (B) CFT in the molar ratio of 0 (a), 1 (b), 5 (c), 10 (d) with BSA.

for DCF and CFT are $(6.18 \pm 0.02) \times 10^5$ and $(4.50 \pm 0.01) \times 10^4$, respectively. The average fluorescence life time of BSA is 5.9 ns as calculated from the fluorescence lifetime measurements, which gives the value of k_Q in the presence of DCF and CFT as 1.04×10^{14} and 9.75×10^{12} L mol^{-1} s^{-1}, respectively. Since these values are fairly larger than limiting diffusion coefficient, K_{dif}, hence one may conclude that the quenching of BSA observed in the presence of DCF and CFT is mainly static by formation of drug–BSA complex (Papadopoulou et al., 2005) and that the interactions between the drug molecules and BSA are specific. However, the fluorescence lifetime measurements performed in the case of DCF clearly show that the quenching is not purely static and there is a fair contribution of the dynamic component in the observed quenching.

Further, the number of binding sites and the association constant for the binding interactions were also calculated using the following equations (Xie et al., 2005),

$$\log\left(\frac{F_0 - F}{F}\right) = \log K_A + n \log[Q] \quad (3)$$

where, K_A and n are the association constant and the number of binding sites respectively. On fitting the quenching data to Eq. (4), for BSA–DCF system, the value of $n = 1.02 \pm 0.10$ ($R = 0.985$) and that for CFT, $n = 1.04 \pm 0.04$ ($R = 0.996$) were obtained. For $n \approx 1$, Eq. (3) can be rewritten as,

$$\frac{F_0}{F_0 - F} = 1 + K_A^{-1}[\mathrm{Q}]^{-1} \quad (4)$$

The slope of the double reciprocal plot of $F_0/(F_0 - \mathrm{F})$ versus $[\mathrm{Q}]^{-1}$ gives the value of the association constant K_A for the binding of BSA with the drugs. In the presence of DCF, the value of association constant, K_A is 8.8×10^5 M^{-1} and that in the presence of CFT is 2.06×10^4 M^{-1}. On comparing these values with those obtained in the ITC experiments at 25 °C, it is clear that for DCF the values do not match whereas for CFT the values are comparable. This result is corroborated by the higher extent of dynamic quenching for BSA observed in the presence of DCF. Thus, it is obvious to expect contradicting values of the binding constant measured through fluorescence based on the assumption of purely static quenching, in the case of DCF. In case of CFT, the results also show that it is reasonable to fix $N = 1$, during the fitting of the integrated heat profiles to a single set of binding site model, for the analysis of CFT–BSA binding because with $N = 1$, the binding constant obtained from fluorescence quenching experiments match closely to that obtained by ITC experiments.

3.6. Circular dichroism spectroscopy

The changes in the secondary and tertiary structures of the protein in the presence of the drugs were studied in the far UV CD and near UV CD regions at the increasing molar ratios of [drug]/[BSA] (Figs. 9 and 10).

In the presence of DCF, the secondary structure of BSA is not affected significantly, since the two minima observed at 209 and 222 nm for the intact protein do not show enough variation with increasing [DCF]/[BSA] ratio. The tertiary structure estimated by the near UV CD spectrum, exhibit cotton effect (Fig 9) which is known to exist in the presence of DCF (Chamouard et al., 1985) and shows a variation as drug concentration goes up.

In the presence of increasing concentrations of CFT, no appreciable conformational changes in the secondary structure of the protein is observed (Fig. 10), even though the tertiary structure is slightly affected by the increasing concentration of the drug. These observations show that the drugs have a small influence on the tertiary conformation of the protein. However, they do not cause any significant alterations in the secondary structure of BSA upon binding.

3.7. Mode of interaction of DCF and CFT with BSA

The ITC experiments for the binding of DCF and CFT in the presence of NaCl and surfactants make it clear that the mode of interaction of these two drugs with BSA is not the same. A reduction in the binding affinity of CFT to BSA with increase in ionic strength indicates predominance of electrostatic interactions in the complexation. However, the binding affinity of DCF for BSA is not significantly altered which suggests more involvement of non-coulombic interactions in the binding process.

The involvement of ionic interactions in the binding of CFT and DCF to BSA is further supported by an absence of typical binding pattern in the presence of SDS which can block the binding sites for the drugs via electrostatic interactions in addition to its ability to partially denature the protein. Similar behavior is observed at both pre- and post-micellar concentrations of surfactants suggesting that both electrostatic and hydrophobic interactions have a role in the binding process.

Being a neutral molecule TX-100 will not interfere in the electrostatic interactions between the drug and the protein. In the pre-micellar concentration of TX-100, no significant changes in the binding affinity of DCF with BSA is observed. However, in the post-micellar concentration, TX-100 can partially alter the protein conformation so as to accommodate DCF with higher affinity due to stronger hydrophobic interactions.

For CFT, the binding affinity decreases only slightly in the presence of both pre- and post-micellar concentrations of TX-100. This suggests that the binding interaction between CFT and BSA is largely electrostatic in nature, which is not affected on addition of uncharged TX-100 but is hindered on addition of a negatively charged SDS.

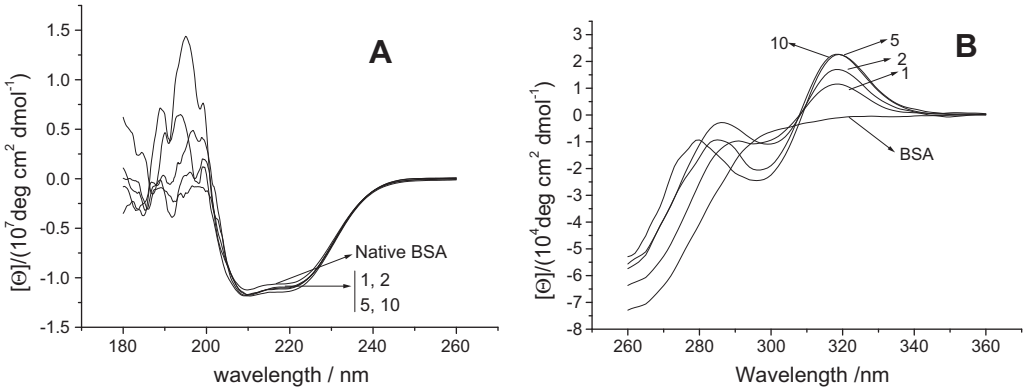

Fig. 9. Circular dichroism (CD) spectra of BSA in the presence of DCF: (A) far-UV CD spectrum and (B) near-UV CD spectrum. The concentrations used are represented as [DCF]/[BSA] molar ratios (1, 2, 5 and 10).

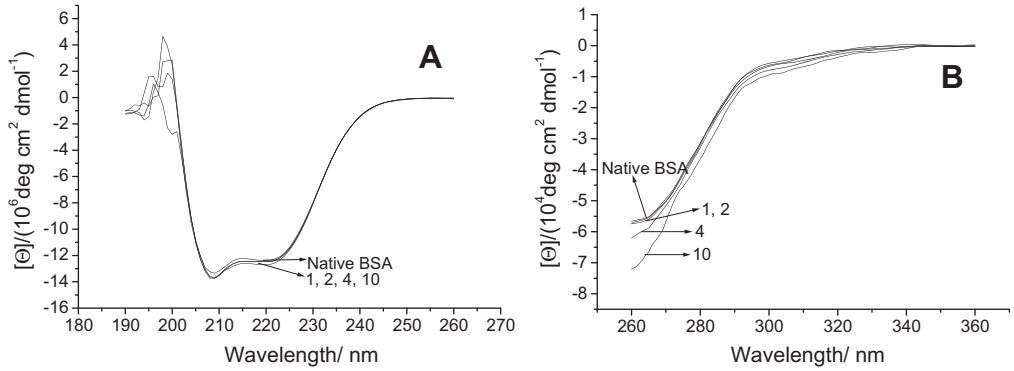

Fig. 10. Circular dichroism (CD) spectra of BSA in the presence of CFT: (A) far-UV CD spectrum and (B) near-UV CD spectrum. The concentrations used are represented as [DCF]/[BSA] molar ratios (1, 2, 4 and 10).

Two binding sites have been reported (Chamouard et al., 1985) for the binding of DCF with serum albumin, with the high affinity binding site being the benzodiazepine binding site and the low affinity binding site being common with the warfarin site. Contrary to this, we found that the ITC data in our experiments fitted well to a single set of binding sites model, with a moderate affinity constant ($\sim 10^4\ M^{-1}$). According to the features described by Sudlow et al., 1975, which allow ligand binding to the specific sites, the aromatic carboxylic acids, with a negative charge specifically located at one end of the molecule, away from the nonpolar region, should bind to site II. Taking this into consideration we propose that DCF binds to BSA at site II which is the benzodiazepine binding site.

A series of binding studies with various cephalosporins and HSA have been carried out (Nerli et al., 1997) using ultrafiltration method where they have reported a binding constant of the order of 10^3 for the binding of CFT to the serum albumin. They have shown through fluorescence studies that CFT is capable of replacing bilirubin from HSA, suggesting bilirubin binding site to be the site where CFT possibly binds. It has been suggested that one part of bilirubin binding site overlaps Sudlow site I (Jackobson, 1969) which usually binds more bulky heterocyclic drug molecules (Sudlow et al., 1975). Our studies on CFT and BSA show a binding constant of the order of 10^4 fitting to a single set of binding sites model. This indicates that it is possible that CFT binds to BSA at site I. Moreover, since the two drugs DCF and CFT, do not interfere with each other in binding with BSA, it suggests that they bind at two different binding sites, with DCF binding at Sudlow site II and CFT binding at Sudlow site I on BSA.

4. Conclusions

The anti-inflammatory drug DCF and antibiotic drug CFT binds to BSA with an affinity constant of the order of 10^4, the former being stronger. The values of binding constant (K), binding enthalpy (ΔH) and binding entropy (ΔS) have been determined using isothermal titration calorimetry. The effect of ionic strength, cationic, anionic and non-ionic surfactants on the binding of DCF and CFT with BSA suggest involvement of both electrostatic and hydrophobic interactions in the binding process. The studies also suggest relatively larger involvement of non-columbic interactions in the binding of DCF to BSA compared to that of CFT. Combinatorial studies of the binding of these drugs suggest that DCF and CFT bind to BSA at two different binding sites. The fluorescence spectroscopic results have helped in understanding the intrinsic details of the binding of these drugs with BSA and the possible binding sites. The differential scanning calorimetric results support tighter binding of DCF wit BSA compared to that of CFT and provide a quantitative measure of the thermal stability of the protein in the presence of these drugs.

Acknowledgments

This work has been sponsored by Department of science and Technology, New Delhi. R.S. and S.C. are supported by fellowships from CSIR, New Delhi.

Appendix A. Supplementary data

Supplementary data associated with this article can be found, in the online version, at http://dx.doi.org/10.1016/j.ejps.2012.03.007.

References

Barcelo, F., Portugal, J., 2004. Elsamicin A binding to DNA; a comparative thermodynamic characterization. FEBS Lett. 576, 68–72.

Briand, C., Sarrazin, M., Peyrot, R., Bourdeaux, M., Sari, J.C., 1982. Study of the interaction between human serum albumin and some cephalosporins. Mol. Pharmacol. 21, 92–99.

Brodersen, R., Honore, B., Pedersen, A.O., Klotz, I.M., 1988. Binding constants for ligand–carrier complexes. Trends Pharmacol. Sci. 9, 252–257.

Brogden, R.N., Heel, R.C., Pakes, G.E., Speight, T.M., Avery, G.S., 1980. Diclofenac sodium: a review of its pharmacological properties and therapeutic use in rheumatic diseases and pain of varying origin. Drugs 20, 24–48.

Carter, D.C., Ho, J.X., 1994. Structure of serum albumin. Adv. Prot. Chem. 45, 153–203.

Catella-Lawson, F., Reilly, M.P., Kapoor, S.C., 2001. Cyclooxygenase inhibitors and the antiplatelet effects of aspirin. New Eng. J. Med. 345, 1809–1817.

Chamouard, J.M., Barre, J., Urien, S., Houin, G., Tillement, J.P., 1985. Diclofenac binding to albumin and lipoproteins in human serum. Biochem. Pharmacol. 34, 1695–1700.

Dutta, S.K., Basu, S.K., Sen, K.K., 2006. Binding of diclofenac sodium with bovine serum albumin at different temperature, pH and ionic strength. Indian J. Exp. Biol. 44, 123–127.

Eftink, M.R., Ghiron, C.A., 1976. Fluorescence quenching of indole and model micelle systems. J. Phys. Chem. 80, 486–493.

Fehske, K.J., Muller, W.E., Wollert, U., 1981. The location of drug binding sites in human serum albumin. Biochem. Pharmacol. 30, 687–692.

Gelamo, E.L., Tabak, M., 2000. Spectroscopic studies on the interaction of bovine (BSA) and human (HSA) serum albumins with ionic surfactants. Spectrochim. Acta Part A: Mol. Biomol. Spectrosc. 56A, 2255–2271.

Gelamo, E.L., Silva, C.H.T.P., Imasato, H., Tabak, M., 2002. Interaction of bovine (BSA) and human (HSA) serum albumins with ionic surfactants: spectroscopy and modeling. Biochim. Biophys. Acta 1594, 84–99.

Goldberg, R.N., Kishore, N., Lennen, R.M., 2002. CRC Handbook of Chemistry and Physics. In: Lide, D.R. (Ed.), 83rd ed. 83rd ed. CRC Press, Boca Raton, FL, pp. 7:12–7:14.

He, X.M., Carter, D.C., 1992. Atomic structure and chemistry of human serum albumin. Nature 358, 209–215.

Jackobson, J., 1969. Binding of bilirubin to human serum albumin: determination of the dissociation constants. FEBS Lett. 5, 112–114.

Jobin, F., Gagnon, F.T., 1971. Inhibition of human platelet aggregation by a dibenzazepine compound (GP 44296) and by N-(2,6-dichlorophenyl)-o-aminophenylacetic acid(GP 45840). Can. J. Physiol. Pharmacol. 49, 479–481.

Joly, V., Pangon, B., Brion, N., Vallois, J.M., Carbon, C., 1998. Enhancement of the therapeutic effect of cephalosporins in experimental endocarditis by altering their pharmacokinetics with diclofenac. J. Pharm. Exp. Ther. 246, 695–700.

Kamat, B.P., Seetharamappa, J., 2005. Study of the interaction between fluoroquinolones and bovine serum albumin. J. Chem. Sci. 11, 649–655.

Kenawi, I.M., Barsoum, B.N., Youssef, M.A., 2005. Drug–drug interaction between diclofenac, cetirizine and ranitidine. J. Pharm. Biomed. Anal. 37, 655–661.

Kenawi, I.M., 2006. DFT analysis of diclofenac activity and cation type influence on the theoretical parameters of some diclofenac complexes. J. Mol. Struct.: Theochem 761, 151–157.

Kragh-Hansen, U., Hellec, F., Foresta, B.D., Maire, M.L., Moller, J.V., 2001. Detergents as probs of hydrophobic binding cavities in serum albumin and other water soluble proteins. Biophys. J. 80, 2898–2911.

Kratochwil, N.A., Huber, W., Muller, F., Kansy, M., Gerber, P.R., 2002. Predicting plasma protein binding of drugs: a new approach. Biochem. Pharmacol. 64, 1355–1374.

Lehrer, S.S., 1971. Solute perturbation of protein fluorescence: the quenching of the tryptophan fluorescence of model compounds and lysozyme by iodide ion. Biochemistry 10, 3254–3263.

Lopez, O., de la Maza, A., Coderch, L., Lopez-Iglesias, C., Wehrli, E., Parra, J.L., 1998. Direct formation of mixed micelles in the solubilization of phospholipid liposomes by Triton X-100. FEBS Lett. 426, 314–318.

Maitani, Y., Nakagaki, M., Nagai, T., 1991. Determination of the acid dissociation constants in ethanol–water mixtures and partition coefficients for diclofenac. Int. J. Pharm. 74, 105–116.

Mandell, G.L., Sande, M.A., 1990. In: Gilman, A.G., Rale, T.W., Nies, A.S., Taylor, P. (Eds.), Goodman and Gilman's the pharmacological basis of therapeutics, eighth ed. Pergamon Press, New York, pp. 1065–1097.

Markovich, M.N., Avereva, E.V., 1985. Microcalorimetry study of pharmacological complexes. The binding of cephalosporins with human serum albumin. Antibiot. Med. Biotechnol. 30, 916–918.

Marks, M.I., 1991. Bacterial meningitis: an update. Clin. Pediatr. 30, 673–675.

Maurice, R.E., Camillo, A.G., 1981. Fluorescence quenching studies with proteins. Anal. Biochem. 114, 199–212.

McNamara, P., Treub, V., Stoeckel, K., 1990. Ceftriaxone binding to human serum albumin. Indirect displacement by probenecid and diazepam. Biochem. Pharmacol. 40, 1247–1253.

Moser, P., Sallmann, A., Wiesenberg, I., 1990. Synthesis and quantitative structure-activity relationships of diclofenac analogues. J. Med. Chem. 33, 2358–2368.

Muller, W.E., Wollert, U., 1979. Human serum albumin as a 'silent receptor' for drugs and endogenous substances. Pharmacology 19, 59–67.

Nerli, B., Romanini, D., Pico, G., 1997. Structural specificity requirements in the binding of beta lactam antibiotics to human serum albumin. Chem. Biol. Interact. 104, 179–202.

Palomo, M.E., Ballesteros, M.P., Frutos, P., 1999. Analysis of diclofenac sodium and derivatives. J. Pharm. Biomed. Anal. 21, 83–94.

Papadopoulou, A., Green, R.J., Frazier, R.A., 2005. Interaction of flavonoids with bovine serum albumin: a fluorescence quenching study. J. Agric. Food Chem. 53, 158–163.

Peters Jr., T., 1996. All About Albumin. Acad. Press, San Diego.

Rahman, M.H., Yamasaki, K., Shin, Y.H., Lin, C.C., Otagiri, M., 1993. Characterization of high affinity binding sites of non-steroidal anti-inflammatory drugs with respect to site-specific probes on human serum albumin. Biol. Pharm. Bull. 16, 1169–1174.

Record, M.T., Anderson, C.F., Lohman, T.M., 1978. Thermodynamic analysis of ion effects on the binding and conformational equilibria of proteins and nucleic acids: the roles of ion association or release, screening and ion effects on water activity. FEBS Lett. 11, 103–178.

Rocca, B., Petrucci, G., 2012. Variability in the responsiveness to low-dose aspirin: pharmacological and disease-related mechanisms. Thrombosis 2012, 1–11.

Sjoholm, I., Ekman, B., Kober, A., Pahlman, I.L., Seiving, B., Sjodin, T., 1979. Binding of drugs to human serum albumin: XI. The specificity of three binding sites as studied with albumin immobilized in microparticles. Mol. Pharmacol. 16, 767–777.

Sober, H.A., Harte, R.A., 1973, second ed. second ed. CRC Press, Cleveland, OH, p. C-71.

Sudlow, G., Birkett, D.J., Wade, D.N., 1975. The characterization of two specific drug binding sites on human serum albumin. Mol. Pharmacol. 11, 824–834.

Sudlow, G., Birkett, D.J., Wade, D.N., 1976. Further characterization of specific drug binding sites on human serum albumin. Mol. Pharmacol. 12, 1052–1061.

Sugio, S., Kashima, A., Mochizuki, S., Noda, M., Kobayashi, K., 1999. Crystal structure of human serum albumin at 2.5 A resolution. Protein Eng. 12, 439–446.

Takeda, K., Shigeta, M., Aoki, K., 1987. Secondary structures of bovine serum albumin in anionic and cationic surfactant solutions. J. Colloid Interface Sci. 117, 120–126.

Tawara, S., Matsumoto, S., Matsumoto, Y., Kamimura, T., Goto, S., 1992. Structure binding relationship and binding sites of cephalosporins in human serum albumin. J. Antibiot. 45, 1346–1357.

Tsivou, E., Melakopoulos, I., Kotsiou, A., Anagnostopoulou, S., Tesseromatis, C., 2005. Alterations in cefalosporin levels in the serum and mandible of hyperlipaedemic rats after co-administration of ibuprofen. Eur. J. Drug Metab. Pharmacokinet. 30, 171–174.

Xie, M.X., Xu, X.Y., Wang, Y.D., 2005. Interaction between hesperetin and human serum albumin revealed by spectroscopic methods. Biochim. Biophys. Acta 1724, 215–224.